

# Comparison of reversible melting behaviour of poly(3-hydroxybutyrate) using quasi-isothermal and other modulated temperature differential scanning calorimetry techniques

R. A. Shanks · L. M. W. K. Gunaratne

Received: 11 July 2010/Accepted: 3 January 2011/Published online: 27 February 2011  
© Akadémiai Kiadó, Budapest, Hungary 2011

**Abstract** Melting behaviour of poly(3-hydroxybutyrate) (PHB) has been investigated by conventional DSC and each of several methods of modulated temperature differential scanning calorimetry (mT-DSC) such as heat-cool, iso-scan, step-scan and quasi-isothermal (QI). Thermal properties were investigated after fast and slow cooling crystallisation treatments. Multiple melting peak behaviour was observed for all methods except conventional melting with an average heating rate. Comparison of the mT-DSC data revealed that PHB underwent reversing melting including several reversible events and some non-reversible contributions under the modulation conditions. The main melting of PHB was irreversible, as were crystallisation and annealing, where the crystals can approach equilibrium. The various fusion enthalpy values were measured and they confirmed significant melt-recrystallisation of PHB with different melting conditions. Only the QI method revealed a true reversible contribution.

**Keywords** Biopolymer · Biopolyester · Modulated temperature DSC · Step-scan temperature · Melting · Crystallisation

## Introduction

Much interest has been attached to biosynthesis, physical properties, biodegradation, modification, and utilisation of bacterial polyesters because of their potential applications

as environment friendly materials [1, 2]. They are manufactured via bacterial fermentation and they biodegrade to water and carbon dioxide [3]. Poly(3-hydroxybutyrate) (PHB) comes under the class of poly(hydroxylalkanoates) (PHA). PHA are thermoplastic polymers whose physical properties depend on the structure of the polymer chain and range from hard rigid solids to elastomers. Bacterial PHB having the chemical structure  $[-O-CH-(CH_3)-CH_2-(C=O)-]_n$  shows promise for biopolymer applications, due to its long-term degradation profile and high molar mass, and it has been available under trade name Biopol since the early 1980s [4]. In addition to biosynthesis, PHA have attracted much interest because of their biocompatibility and biodegradability. A number of potential applications have been suggested for PHB in medical, marine and agricultural fields. However, PHB has relatively high melting temperature ( $T_m$ ), to 443 K for the homopolymer [5, 6]. Their relatively high glass transition temperatures ( $T_g$ ) and crystallinity have made them too brittle for many applications.

Differential scanning calorimetry (DSC) is an important technique to study melting and crystallisation behaviour of polymers. The interpretation of DSC results is difficult due to various transformations occurring simultaneously during heating. Modulated temperature differential scanning calorimetry (mT-DSC) has attracted much interest since its development in 1992, because of its ability to distinguish apparent thermodynamic (reversing heat flow) and kinetic (non-reversing heat flow) events under the prevailing DSC modulation conditions [7, 8]. The theory and operating principles have been thoroughly described [7–10]. Three types of curves can be derived from the experiments: total heat flow or isobaric apparent heat capacity curve ( $C_{p,\text{total}}$ ), the same as a conventional DSC curve), the in-phase curve (reversing or storage  $C_p$ ) and out-of-phase curve (loss  $C_p$ )

R. A. Shanks (✉) · L. M. W. K. Gunaratne  
School of Applied Sciences, RMIT University, GPO Box 2476V,  
Melbourne, VIC 3001, Australia  
e-mail: robert.shanks@rmit.edu.au

[11]. In addition, a non-reversing heat capacity (kinetic) curve ( $C_{p, NR}$ ) can be obtained from the difference between the total  $C_p$  and reversing  $C_p$ . For all modulation types, the time-temperature ( $t-T$ ) program can be written as a sum of linear and periodic components ( $T_p$ ) according to Eq. 1

$$T(t) = T_0 + \beta_0 t + T_p(t), \quad (1)$$

where  $T_0$  is the initial temperature and  $\beta_0$  is the average heating rate.

Another mT-DSC method, the called step-scan DSC (SDSC), has recently become available [12]. SDSC utilizes a heating-isothermal (or cooling-isothermal) program, where the isothermal segment continues for a set time and heat flow is decreased to within a predetermined set-value (criteria). The apparent thermodynamic response only occurs during the heating (or cooling) segment and reflects the reversing changes within the sample. The time-dependent response reflects the kinetic processes and is extracted from the isothermal baseline segment. The equation that describes the heat flow response is given by Eq. 2:

$$\frac{dQ}{dt} = C_p \left[ \frac{dT}{dt} \right] + f[t, T] \quad (2)$$

where  $dQ/dt$  is the heat flow,  $C_p$  is the isobaric heat capacity,  $dT/dt$  is the heating rate and  $f(t, T)$  is the kinetic response. The interpretation of results is similar to other forms of mT-DSC. Analysis of the heat flow signal provides two curves: the apparent thermodynamic  $C_p$  ( $C_{p, ATD}$ ) signal (reversible under the experimental conditions, which is called reversing) and the Isok baseline  $C_p$  ( $C_{p, Isok}$ ) (kinetic or non-reversing) curves [13]. Crystallisation and melting of linear macromolecules include irreversible processes [14]. The reversing heat capacity can be interpreted by considering annealing, recrystallisation and secondary crystallisation. Reversing and non-reversing processes have been separated by mT-DSC techniques for a considerable number of semicrystalline polymers, such as poly(ethylene naphthalate) [15], poly(butylene terephthalate) [16], poly( $\epsilon$ -caprolactone) [17], linear low-density polyethylene [18], polypropylene [19], polyethylene [20] and poly(ethylene-2-6-naphthalene dicarboxylate)-poly(ethylene terephthalate) [21] blends.

Six contributions to the thermodynamic and apparent heat capacity have been reported in the melting and crystallisation regimes [18, 20, 22]. The reversible contributions are (1) the vibrational heat capacity, (2) the latent heat of molecules or parts of molecules that truly melt reversibly and (3) the equilibrium of conformational defects. The irreversible contributions are all latent heat influences in the form of (4) primary crystallisation, (5) secondary crystallisation and (6) crystal perfection.

Reversible melting involves a small amount of material and it takes place at the interface between crystals and

melts. Researchers suggested that the molar mass plays a primary role in reversible melting [20]. Short molecules need only primary nucleation to crystallise. But, long molecules may have some segments partially attached to crystals. The partially melted molecules reversibly recrystallise during the cooling step of the heat-cool processes of mT-DSC experiments. Formation of spherulites after primary nucleation can be generated by molecular nucleation [23]. Reversible melting is due to melting and crystallisation on lateral crystal surfaces by decoupled chain segments of the polymer. Polymers are macromolecules and to study their rearrangement requires more time due to restricted mobility [24]. Therefore, modulated temperature programs, in particular quasi-isothermal (QI) modulated temperature calorimetry, play an important role in investigation of molecular nucleation. Using QI modulation at a constant temperature can reduce reversing heat capacity of polymers in the melting region. Heat capacity analysis by QI has been discussed elsewhere [25, 26]. Truly reversible heat capacity can be obtained by increasing the experimental time until a steady state is reached and accurate heat capacities can be calculated by this method. The QI experiments provide the truly reversible melting component without other irreversible processes such as recrystallisation, annealing and melting [11]. The QI technique has been used to analyse reversible melting behaviour of polymers and co-polymers, such as polyethylene [20], polypropylene [27], poly[carbonyl(ethylene)-co-poly(propylene)] [22], poly(ethylene-*co*-octene) [18], poly(oligoamide-*alt*-oligoether) [28] and linear low-density polyethylene [29].

The aim is to investigate true reversible melting behaviour of PHB and to compare mT-DSC techniques. The reversing melting behaviour of PHB was analyzed using mT-DSC: heat-cool, iso-scan, step-scan and QI methods. It is necessary to use a QI method to measure true reversible melting effects (slow time-dependent processes within the material) [25, 26]. It is interesting to understand that the reversible process may be slower than the instrument response to the selected modulation. Therefore, it is important to select slower frequencies of modulation to enhance outcome of experiments.

## Experimental

### Materials and preparation

Bacterial PHB of  $M_w = 2.3 \times 10^5$  g mol<sup>-1</sup> and  $M_n = 8.7 \times 10^4$  g mol<sup>-1</sup> was purchased from Sigma-Aldrich Chemicals as a white powder [30]. PHB (1 g) was dissolved in 100 mL of chloroform and filtered by vacuum filtration to remove an insoluble fraction or impurities.

Semicrystalline films were obtained by solvent casting at room temperature. The resulting films ( $\sim 60 \mu\text{m}$  thick) were further dried under vacuum at 323 K for 3 h to remove residual solvent and moisture. Films were stored in a desiccator under nitrogen atmosphere prior to use.

#### Differential scanning calorimetry

All measurements and thermal treatments were performed using a Perkin-Elmer series Pyris 1 DSC (Pyris software 7) operated using subambient temperature cooling with an Intracooler 2P so that heat-cool program response would be more precise. About 2–3 mg of polymer was accurately weighed using a Mettler UMX5 microbalance for each scan, sealed in 10  $\mu\text{L}$  aluminium pans, and all scans were carried out under inert nitrogen (20  $\text{mL min}^{-1}$ ). High purity indium and octadecane were used for temperature calibration, and indium standard was used for calibration of heat flow. The furnace was calibrated according to the manufacturers' recommendation. Specific heat capacity calibrations were confirmed using a sapphire standard.

DSC melting scans were obtained using a heating rate of 10  $\text{K min}^{-1}$  from 253 to 463 K. For each type of scan, a baseline was recorded with matched empty aluminium pans using the same method. From the DSC heating scans, glass transition temperature ( $T_g$ ), cold crystallisation temperature ( $T_{cc}$ ), melting temperature ( $T_m$ ) and enthalpy of fusion ( $\Delta H_m$ ) were determined.  $T_g$  was measured at the half-height of the glass transition inflection. Crystallization and melting temperatures were measured at the peak temperatures, and enthalpy was measured from the area under the respective crystallization exotherm or melting endotherm. The crystallinity was calculated using Eq. 3,

$$X_{c,\text{PHB-RPLA}} = \Delta H_{\text{PHB-RPLA}} / \Delta H_{\text{PHB}}^0, \quad (3)$$

where  $\Delta H_{\text{PHB}}^0$  is the enthalpy of melting of pure crystals 146  $\text{J g}^{-1}$  [31]. PHB films were treated continuous cooling condition at rate of 200  $\text{K min}^{-1}$  (to minimise crystallisation) and 2  $\text{K min}^{-1}$  (reasonable time for crystallisation) from 463 to 253 K. Before the treatment, polymers were heated to 463 K at 40  $\text{K min}^{-1}$  and held for 3 min to destroy any previous thermal history.

#### mT-DSC method and data analysis

mT-DSC melting scans were obtained by using a heat-cool modulation from 253 to 463 K. The heat-cool program used linear segments of heating and cooling with heating rate of 6  $\text{K min}^{-1}$  for 30 s followed by cooling at 2  $\text{K min}^{-1}$  for 30 s, respectively. The iso-scan program of linear segments of heating and isothermal with a heating rate of 4  $\text{K min}^{-1}$  for 30 s followed by isothermal for 30 s. Both of these programs provided a frequency of 16.7 mHz

(period = 60 s), an average cooling rate of 2  $\text{K min}^{-1}$  and a temperature amplitude of 1 K for heat-cool and 0.5 K for iso-scan. The heat flow data from the mT-DSC scans were then used to calculate the total heat capacity ( $C_{p,\text{total}}$ ) and storage or reversing heat capacity ( $C_p'$ ). From the mT-DSC heating scans, melting temperature ( $T_m$ ) and enthalpy of fusion ( $\Delta H_m$ ) were determined. PHB films were treated by a continuous cooling condition at a rate of 2  $\text{K min}^{-1}$  from 443 to 253 K to minimise crystallisation. Before the treatment, polymers were heated to 443 K at 40  $\text{K min}^{-1}$  and held for 3 min to destroy any previous thermal history.

#### SDSC method

The SDSC melting scan of PHB with controlled thermal history was obtained with an average heating rate of 2  $\text{K min}^{-1}$  and a period of 60 s (a temperature increment of 2 K with each 30 s scanning segments) from 253 to 463 K. The PHB was treated by cooling at 2  $\text{K min}^{-1}$ . Heat capacity calculation from heat flow response of the SDSC scans was carried out using the area method. The data for each isothermal segment were collected to within a 0.005-mW baseline criteria. Our preliminary investigations proved that these were suitable experimental parameters for the relevant polymers. The heat flow data from the SDSC scans were used to calculate the apparent thermodynamic heat capacity and IsoK baseline as a heat capacity. From the SDSC heating scan, melting temperature and enthalpy of fusion were determined.

#### Quasi-isothermal mT-DSC

The QI mode melting scans were obtained at various temperatures between 253 and 463 K every 2–10 K steps, to observe behaviours during transition regions smaller temperature intervals were selected (263–283 K and 403–453 K); modulation parameters were underlying heating rate of 0  $\text{K min}^{-1}$ , temperature amplitude 0.5 K, period 60 s and 20 min time; the last 10 min modulation data were used for the calculation.

Heat-cool mT-DSC scans were performed at an underlying heating rate of 0  $\text{K min}^{-1}$  with period 60 s (frequency 16.7 mHz) and modulated temperature amplitude of 0.5 K. The numbers of repetitions were limited to 20 modulation cycles at a constant temperature. The data for the last 10 min were taken for calculation of results at selected temperatures to minimise distortion, and the heat capacity was plotted for each temperature. PHB was treated using continuous slow and fast cooling at rates of 2 and 200  $\text{K min}^{-1}$ , respectively, from 463 to 253 K before measurement. A baseline was recorded with matched empty aluminium pans for each type of scan using the same scan parameters. mT-DSC curves were corrected using the

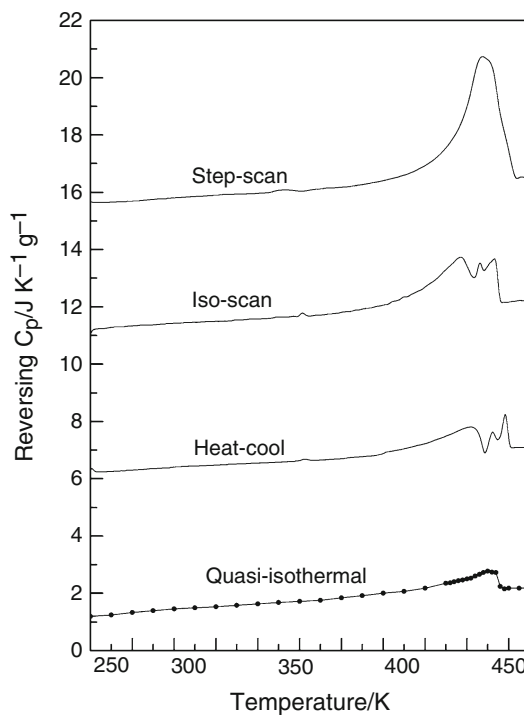


**Fig. 1** Reversing  $C_p$  curves from various mT-DSC programs (indicated on curves; the three upper curves have each been shifted by 5 units)

appropriate baselines recorded under identical conditions and converted to heat capacity curves.

## Results and discussion

### Evaluation of mT-DSC reversing contributions

The reversing melting behaviour of PHB was investigated under various conditions. Figure 1 shows reversing heat capacity curves obtained from the various mT-DSC methods: QI, heat-cool, iso-scan and step-scan after  $2 \text{ K min}^{-1}$  cool. An average heating rate of  $2 \text{ K min}^{-1}$  was used for all curves except QI. The  $2 \text{ K min}^{-1}$  heating rate used was regarded as a relatively slow scan rate and at that rate PHB molecules would have enough time to undergo re-crystallization during melting. The melting temperatures ( $T_m$ ) and heat of fusions ( $\Delta H_m$ ) obtained from various methods are listed in Table 1.

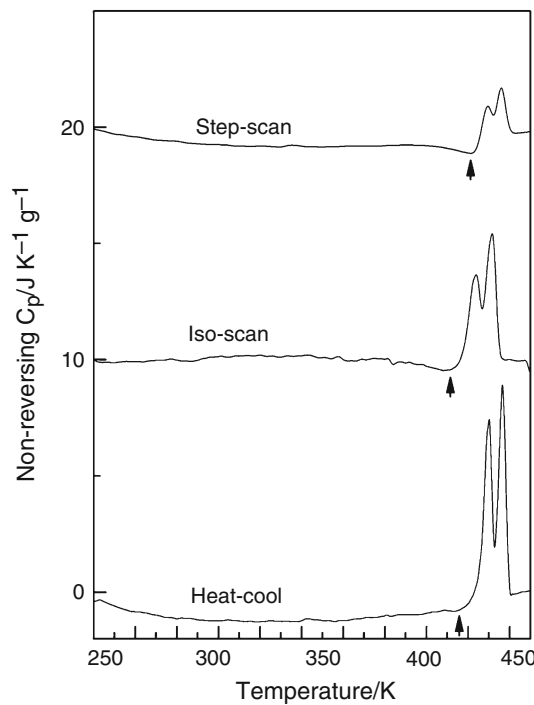
These reversing melting curves exhibited overlapped double melting endotherms from SDSC and QI curves and overlapped triple melting peaks from heat-cool and iso-scan mT-DSC, suggesting the presence of melting recrystallisation and remelting (mrr) processes. Nevertheless, the PHB analysed by the mT-DSC heat-cool program gave better resolved melting peaks that appeared at about 435, 445 and 451 K, while the melting peaks obtained from the

**Table 1** Reversing melting data of PHB after different melting conditions

Method	$T_m (C_p')/\text{K}$	$\Delta H_m (C_p')/\text{J g}^{-1}$
Quasi isothermal	429.0, 445.0	0.9
Heat-cool	435.1, 445.2, 451.4	26.0
Iso-scan	430.3, 439.1, 446.0	49.0
Step-scan	440.5, 443.4	98.2

iso-scan program showed much broader peaks (430, 439 and 446 K) at lower temperatures. A cooling component of each cycle provides better resolution of reversing and non-reversing events than a heating only temperature modulation, where the non-reversing events can only manifest in the isothermal regime.

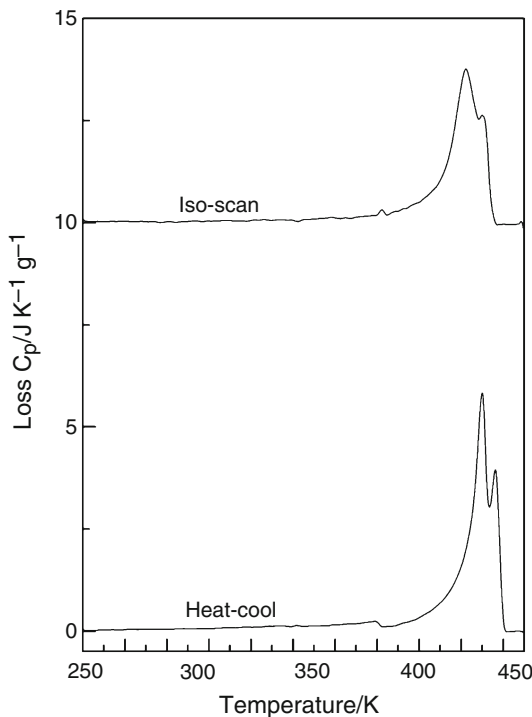
The melting curve analysed by step-scan DSC heating program exhibits a broad peak that contains two largely overlapped melting peaks (429 and 443 K), indicative of significant recrystallisation during melting. The lowest melting enthalpy value of  $0.9 \text{ J g}^{-1}$  was obtained from QI reversing contribution, whereas the step-scan reversing  $C_p$  curve provided the highest value of  $98.2 \text{ J g}^{-1}$ . The enthalpy of fusion was higher for the modulated heating scans (Table 1), suggesting re-crystallisation and/or annealing of crystals during the isothermal equilibration part of the



**Fig. 2** Non-reversing  $C_p$  curves from various mT-DSC programs (indicated on curves; the three upper curves have each been shifted by 10 units)

**Table 2** Non-reversing and loss melting data of PHB after different melting conditions

Method	$T_m(C_{p,NR})/K$	$\Delta H_m(C_{p,NR})/J\ g^{-1}$	$T_m(C_p'')/K$	$\Delta H_m(C_p'')/J\ g^{-1}$
Heat-cool	443.2, 449.6	63.8	443.0, 449.2	79.8
Iso-scan	437.1, 444.7	46.1	435.2, 443.2	71.0
Step-scan	442.5, 449.0	14.5	—	—

**Fig. 3** Loss  $C_p$  curves from various mT-DSC programs (indicated on curves; the three upper curves have each been shifted by 10 units)

modulation cycles, so that some PHB that has already melted can recrystallise, then melt again. The reversing curves characterised all of the reversible events and some non-reversible contributions due to the modulation conditions only providing an approach to mrr equilibrium. Unstable crystals contribute to melting that is reversible and apparent in the reversing  $C_p$  curve. It has been known that poorly crystallised polymers have a larger reversing melting contribution and smaller non-reversing contribution, while perfect crystals show almost no reversing and larger non-reversing contributions [9]. Analogous results have been reported for the mT-DSC studies of poly(ethylene succinate) and poly(butylene succinate) by Qiu et al. [32]. The SDSC technique has been rarely reported, though useful data interpretation been recently discussed by Liska et al. [33].

The reversing heat capacity curve contains the rapidly reversing (or in-phase) component of the total heat capacity, while the non-reversing curve represents irreversible component of the total heat capacity over the time and

temperature of the modulation. Exothermic crystallisation peaks were not observed in these curves as crystallisation provided a non-reversing contribution. Endothermic melting can be detected in both reversing and non-reversing heat capacity curves. However, exothermic behaviour was detected only in the non-reversing heat capacity curve because the slow kinetics caused a heat flow response that was not in-phase with the temperature oscillation [9].

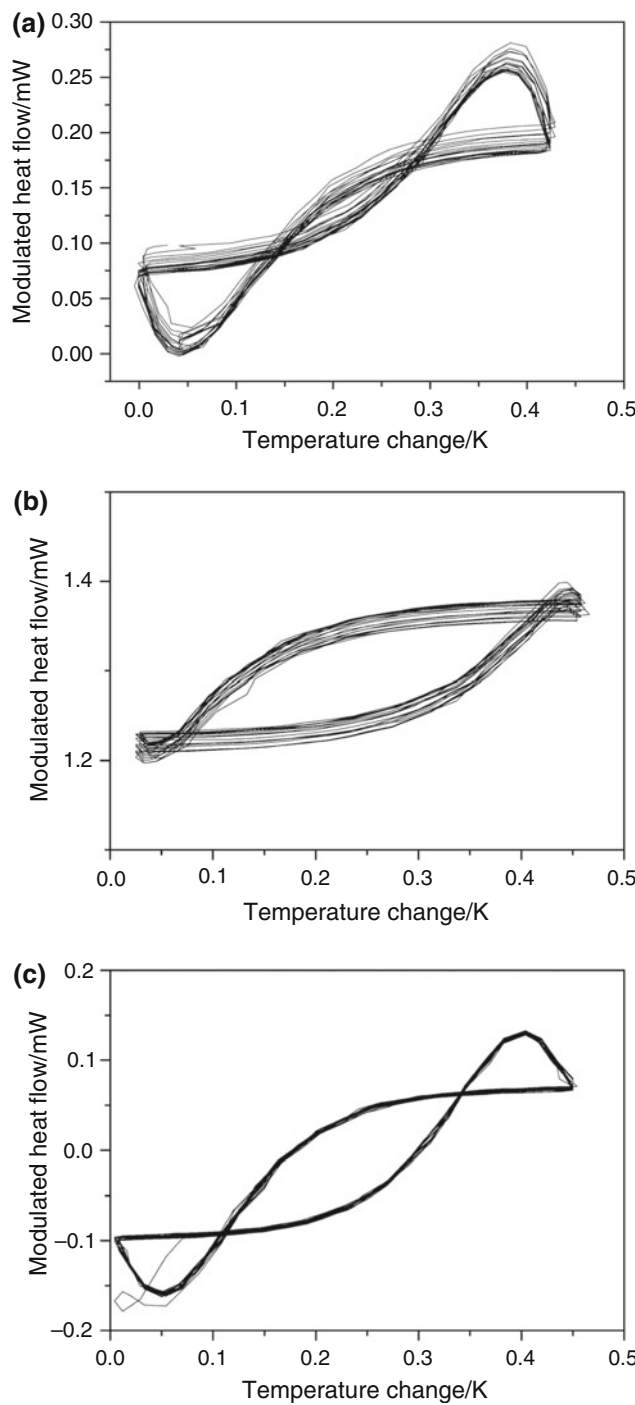
#### Evaluation of mT-DSC non-reversing and loss contributions

The non-reversing contributions of PHB under various conditions are shown in Fig. 2, and relevant thermal data are listed in Table 2. All  $C_{p,NR}$  curves show a broad exothermic peak before melting (indicated by arrow) and two melting peaks. The exothermic only or both exothermic and endothermic behaviour of  $C_{p,NR}$  curve has been reported for polyethylene [34]. The exothermic non-reversing contribution of PHB showed significant recrystallisation and/or annealing during the heating process. The recrystallisation exotherm was impossible to observe in the conventional DSC scan due to the offset of re-crystallisation exotherm and melting endotherm.

The loss  $C_p$  curves of PHB are shown in Fig. 3, and corresponding thermal data are listed in Table 2. The loss  $C_p(C_p'')$  curves represent the irreversible contribution during the modulation and are part of the  $C_{p,NR}$  curve. These curves show zero baselines up to 393 K, suggesting there is no structural change involved before that temperature. The loss  $C_p$  peaks represent entropy gained during disruption of the crystalline structure. The physical meaning of the loss  $C_p$  has been associated with entropy changes during experimental time changes [35].

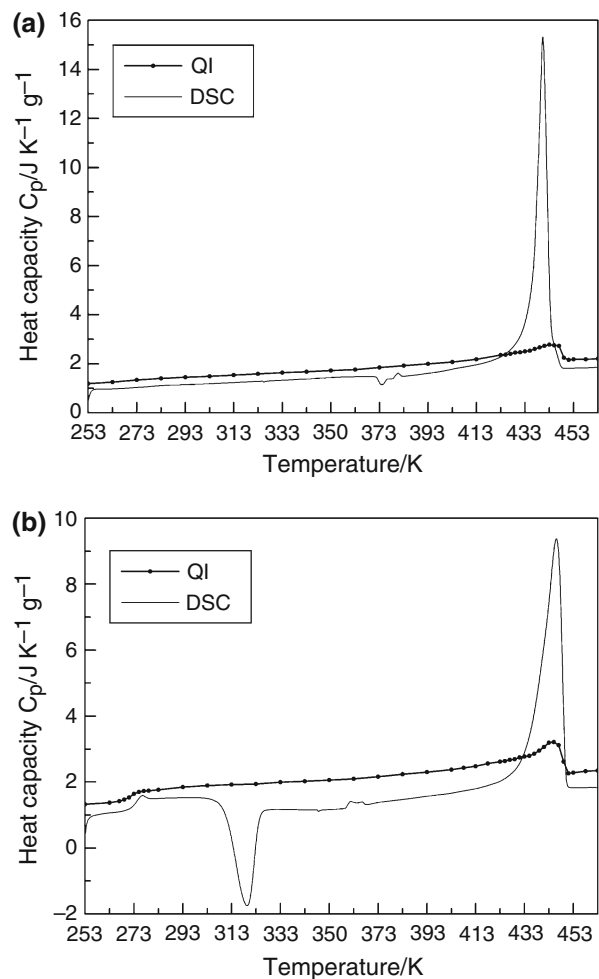
#### Quasi-isothermal mT-DSC analysis

Figure 4a–c shows Lissajous figures of PHB at starting at 293, 323 and 443 K, respectively. Twenty modulations were used for all QI experiments. The Lissajous figure from 323 K shows rearrangement of molecules and the Lissajous figure from 443 K shows melting of crystals with the data approximating linear response. Linear response and steady-state are theoretical requirements for mT-DSC.



**Fig. 4** Lissajous figures for quasi-isothermal experiments on PHB from **a** 293 K, **b** 323 K and **c** 443 K

Steady-state over a cycle is not achieved during re-crystallisation and melting since the morphology of the sample is changing, however, steady state is approximated by having several modulation cycles over each thermal event. Heat flow curves were overlapped from 443 K since the melt was at thermal equilibrium so that subsequent cycles superimposed confirming linear response.



**Fig. 5** Quasi-isothermal modulated and standard DSC heat capacity curves after **a**  $2 \text{ K min}^{-1}$ , **b**  $200 \text{ K min}^{-1}$  cooling of PHB; the thin line represents the standard DSC curve obtained at  $10 \text{ K min}^{-1}$

The reversing curves characterised all of the reversible events and some non-reversing contributions under the modulations conditions. QI has recently been introduced to obtain true reversible events [18, 27, 29, 36]. The QI heat capacity data, obtained at various selected temperatures between 253 and 463 K after modulation for 20 min at a constant temperature, for PHB are shown in Fig. 5a and b and corresponding results are listed in Table 3. At steady state (i.e. after removing all modulation distortions and allowing the sample to equilibrate), the curves show only reversible contributions. Steady state, where data collection commenced, was identified using Lissajous figures [11]. Consideration of heat capacities before and after melting suggests that a small amount of melting was thermodynamically reversible in these regions. Figure 5a shows  $10 \text{ K min}^{-1}$  conventional DSC and QI curves obtained after  $2 \text{ K min}^{-1}$  cooling from 463 to 253 K. A conventional continuous heating DSC curve (thin line) comprises many contributions, including reversible melting.

**Table 3** DSC and QI melting data of PHB after various crystallisation conditions

Polymer	$T_g/K$	$T_c/K$	$\Delta H_c/J\ g^{-1}$	$T_{m1}/K$	$T_{m2}/K$	$\Delta H_m/J\ g^{-1}$	$X_c$
SC2-PHB-DSC10	–	–	–	440.4	445.5	92.5	0.63
SC2-PHB-QI	–	–	–	429.0	443.0	0.9	0.006*
FC200-PHB-DSC10	273.03	319.4	47.9	–	446.1	81.0	0.56
FC200-PHB-QI	271.40	–	–	433.0	445.0	6.3	0.04*

\* Crystallinity was calculated from QI curve

SC2-PHB-DSC10: cool 2 K min<sup>-1</sup>, heat 10 K min<sup>-1</sup>

SC2-PHB-QI: cool 2 K min<sup>-1</sup>, heat quasi-isothermal

FC200-PHB-DSC10: cool 200 K min<sup>-1</sup>, heat 10 K min<sup>-1</sup>

FC200-PHB-QI: cool 200 K min<sup>-1</sup>, heat quasi-isothermal

However, the slow cooled QI curve shows a very low reversible contribution (9.3%) of the total curve within the melting region. Very low reversible melting contributions have been observed for polyethylene [11, 18]. Unresolved double melting peaks at 429 and 443 K were observed in the QI curve. However, the normal DSC curve showed one melting peak and a shoulder at 440 and 445 K, respectively. Furthermore, 10 K min<sup>-1</sup> DSC and QI curves of fast cooled (200 K min<sup>-1</sup>) PHB are shown in Fig. 5b. The continuous heating DSC curve revealed glass transition, cold crystallisation and melting temperatures at 273.03, 319.4 and 446 K, respectively.

The QI curve showed only reversible contributions such as, glass transition at 271.4 K and unresolved double melting peaks at 433 and 445 K. The melting enthalpy of slowly cooled PHB of 0.9 J g<sup>-1</sup> was lower than 6.3 J g<sup>-1</sup> for fast cooled PHB. The enthalpy was calculated by integrating the QI curves over the analysed temperature range. The degree of reversibility was low for slow cooled relatively perfect lamellae of highly crystalline PHB. The results are in agreement with those for high-density polyethylene and low-density polyethylene that had higher enthalpy for fast cooled polymers compared with slow cooled [11]. The higher crystallinity of fast cooled PHB showed a higher degree of reversibility compared with slow cooled perfect lamellae of PHB.

## Conclusions

The mT-DSC results of the PHB strongly depended on prior thermal treatments as well as melting technique. The melting of PHB was complex due to reorganisation and/or recrystallisation during melting. It was found that crystals formed under different crystallisation conditions had varying stability and they showed different amounts of reversing contributions. The reversing curves under various mT-DSC methods exhibited all of the reversible events and

some non-reversible contributions under the various modulations conditions. Only the QI method exhibited the true reversible contribution of PHB melting. The main melting of PHB is irreversible, but some reversible contributions are observed by QI modulated temperature DSC. Crystallisation of PHB is slow and incomplete, while melting is complex due to kinetics of the superimposed melting–recrystallisation–re-melting process. These time–temperature and complex events provide an interesting system for comparison of the set of modulated temperature DSC techniques.

## References

1. Poirier Y, Dennis DE, Nawrath C, Somerville C. Progress toward biologically produced biodegradable thermoplastics. *Adv Mater.* 1993;5:30–7.
2. Cox MK. Studies in polymer science. In: Doi Y, Fukuda K, editors. *Biodegradable plastics and polymers*, vol. 12. Amsterdam: Elsevier; 1994. p. 120–35.
3. Doi Y. *Microbial polyesters*. New York: VCH Publishers; 1990.
4. Holmes PA. Applications of PHB—a microbially produced biodegradable thermoplastic. *Phys Technol.* 1985;16:32–6.
5. El-Hadi A, Schanabel AR, Straube E, Muller EG, Henning S. Correlation between degree of crystallinity, morphology, glass temperature, mechanical properties and biodegradation of poly (3-hydroxyalkanoate) PHAs and their blends. *Polym Test.* 2002;21:665–74.
6. Ha CS, Cho WJ. Miscibility, properties, and biodegradability of microbial polyester containing blends. *Prog Polym Sci.* 2002;27: 759–809.
7. Gill PS, Sauerbrunn SR, Reading M. Modulated differential scanning calorimetry. *J Therm Anal Calorim.* 1993;40:931–9.
8. Schawe JEK. A comparison of different evaluation methods in modulated temperature DSC. *Thermochim Acta.* 1995;260:1–16.
9. Wunderlich B, Okazaki I, Ishikiriyama K, Boller A. Melting by temperature-modulated calorimetry. *Thermochim Acta.* 1998;324: 77–85.
10. Wunderlich B, Boller A, Okazaki I, Ishikiriyama K, Chen W, Pyda M, Pak J, Moon I, Androsch R. Temperature-modulated differential scanning calorimetry of reversible and irreversible first-order transitions. *Thermochim Acta.* 1999;330:21–38.

11. Amarasinghe G, Chen F, Genovese A, Shanks RA. Thermal memory of polyethylenes analyzed by temperature modulated differential scanning calorimetry. *J Appl Polym Sci.* 2003;90:681–92.
12. Gunaratne LMWK, Shanks RA. Isothermal crystallisation kinetics of poly(3-hydroxybutyrate) using step-scan DSC. *J Therm Anal Calorim.* 2006;83:313–9.
13. Pielichowski K, Flejtuch K, Pielichowski J. Step-scan alternating DSC study of melting and crystallisation in poly(ethylene oxide). *Polymer.* 2004;45:1235–42.
14. Wunderlich B. Macromolecular physics, vol. 1. New York: Academic Publishers; 1973.
15. Sauer BB, Kamper WG, Blanchard EN, Threefoot SA, Hsiao BS. Temperature modulated DSC studies of melting and recrystallization in polymers exhibiting multiple endotherms. *Polymer.* 2000;41:1099–108.
16. Righetti MC. Reversible melting in poly(butylene terephthalate). *Thermochim Acta.* 1999;330:131–5.
17. Wurm A, Merzlyakov M, Schick C. Isothermal crystallisation of PCL studied by temperature modulated dynamic mechanical and TMDSC analysis. *J Therm Anal Calorim.* 1999;56:1155–61.
18. Androsch R, Wunderlich B. A study of annealing of poly(ethylene-co-octene) by temperature-modulated and standard differential scanning calorimetry. *Macromolecules.* 1999;32:7238–47.
19. Androsch R, Wunderlich B. Reversible crystallization and melting at the lateral surface of isotactic polypropylene crystals. *Macromolecules.* 2001;34:5950–60.
20. Pak J, Wunderlich B. Melting and crystallization of polyethylene of different molar mass by calorimetry. *Macromolecules.* 2001;34:4492–503.
21. Kampert WG, Sauer BB. Temperature modulated DSC studies of melting and recrystallization in poly(ethylene-2,6-naphthalene dicarboxylate) (PEN) and blends with poly(ethylene terephthalate) (PET). *Polymer.* 2001;42:8703–14.
22. Pyda M, Di Lorenzo ML, Pak J, Kamasa P, Buzin AS, Grebowicz J, Wunderlich BJ. Reversible and irreversible heat capacity of poly[carbonyl(ethylene-co-propylene)] by temperature-modulated calorimetry. *Polym Sci B.* 2001;39:1565–77.
23. Wunderlich B. Molecular nucleation and segregation. *Discuss Faraday Soc.* 1979;68:239–43.
24. Cser F, Hopewell JL, Shanks RA. Reversible melting of thermally fractionated polyethylene. *J Therm Anal.* 1998;54:709–19.
25. Wunderlich B, Jin Y, Boller A. Mathematical description of differential scanning calorimetry based on periodic temperature modulation. *Thermochim Acta.* 1994;238:277–93.
26. Boller A, Jin Y, Wunderlich B. Heat capacity measurement by modulated DSC at constant temperature. *J Therm Anal.* 1994;42:307–30.
27. Genovese A, Shanks RA. Crystallization and melting of isotactic polypropylene in response to temperature modulation. *J Therm Anal.* 2004;75:223–48.
28. Di Lorenzo ML, Pyda M, Wunderlich B. Reversible melting in nanophase-separated poly(oligoamide-alt-oligoether)s and its dependence on sequence length, crystal perfection, and molecular mobility. *J Polym Sci B.* 2001;39:2969–81.
29. Androsch R, Wunderlich B. Analysis of the degree of reversibility of crystallization and melting in poly(ethylene-co-1-octene). *Macromolecules.* 2000;33:9076–89.
30. Zhang LL, Goh SH, Lee SY, Hee GR. Miscibility, melting and crystallization behavior of two bacterial polyester/poly(epichlorohydrin-co-ethylene oxide) blend systems. *Polymer.* 2000;41:1429–39.
31. Gogolewski S, Jovanovic M, Perren SM, Dillon JG, Hughes MK. Tissue response and in vivo degradation of selected polyhydroxyc acids: polylactides (PLA), poly(3-hydroxybutyrate) (PHB), and poly(3-hydroxybutyrate-co-3-hydroxyvalerate) (PHB/VA). *J Biomed Mater Res.* 1993;27:1135–48.
32. Qiu Z, Komura M, Ikehara T, Nishi T. DSC and TMDSC study of melting behaviour of poly(butylene succinate) and poly(ethylene succinate). *Polymer.* 2003;44:7781–5.
33. Liška M, Černošek Z, Chromčíková M, Holubová J, Černošková E, Vozár L. New features of the glass transition revealed by the StepScan® DSC. *J Therm Anal Calorim.* 2010;101:189–94.
34. Scherrenberg R, Mathot V, Hemelrijk AV. The practical applicability of TMDSC to polymeric systems. *Thermochim Acta.* 1999;330:3–19.
35. Garden J, Richard J, Saruyama Y. Entropy production in TMDSC. *J Therm Anal Calorim.* 2008;94:585–90.
36. Amarasinghe G, Shanks RA. TMDSC analysis of single-site copolymer blends after thermal fractionation. *J Therm Anal.* 2004;78:349–61.